Effects of synthesis conditions on ion exchange properties of þÿ±-zirconium phosphate for Eu and Am

Wiikinkoski, Elmo Werneri

2017-12

Wiikinkoski , E W , Harjula , R O , Lehto , J K , Kemell , M L & Koivula , R T 2017 , ' Effects þÿof synthesis conditions on ion exchange properties of ±-zirconium pho þÿ' , Radiochimica Acta , vol. 105 , no. 12 , pp. 1033 1042 . https://doi.

http://hdl.handle.net/10138/243951
https://doi.org/10.1515/ract-2016-2740

unspecified
publishedVersion

Elmo W. Wiikinkoski*, Risto O. Harjula, Jukka K. Lehto, Marianna L. Kemell and Risto T. Koivula

Effects of synthesis conditions on ion exchange properties of α-zirconium phosphate for Eu and Am

DOI 10.1515/ract-2016-2740
Received November 21, 2016; accepted April 6, 2017; published online May 25, 2017

Abstract: Three zirconium phosphate products A, B and C, made through different synthesis routes, were investigated for their europium and americium ion exchange properties utilizing radiotracers $^{152}Eu^{3+}$ and $^{241}Am^{3+}$. Aim of this investigation was to see how material properties change based on different synthesis, and how does the changes effect on trivalent Eu and Am uptake and affinities on the materials. Ultimate goal of an ongoing research is to create inorganic exchanger suitable for separation of trivalent actinides and lanthanides. Powder X-ray diffraction showed that all three products had same α-zirconium phosphate crystal structure. The P:Zr ratio determined by microscope X-ray microanalysis was also the same for all products: 2.43 ± 0.05. However, infrared absorbance, material acidity, particle morphology, and Eu and Am distribution coefficients differed significantly between products. The intensities of the strong IR absorption at approximately 960 cm^{-1}, attributed to vibrations of the orthophosphate group, were in descending order B > C > A. Material acidity showed the same descending order B > C > A. First acidity constants pK_{a1} were 2.3 for product B, 3.1 for C and 3.5 for A. Unit cell volumes increased in the reverse order: B < C < A. Distribution coefficients (K_D), studied for pH 0 to 3 nitric acid media, varied remarkably. For any given pH the K_D descended in the order A > C > B for both Eu and Am. Separation factors, defined as K_D(Eu): K_D(Am), were from 4 to 41 for product A, from 5 to 15 for B, and from 3 to 7 for C. Selectivity coefficients ($k_{M/H}$, M = Eu, Am) and sorption strength decreased along with increasing ZrP product acidity. Metal binding coefficients (k_M) had high values, up to 10^9, especially in ZrP C and A, while the selectivity coefficients were low, 10^{-5} to 10^{-1}, because they relate to the third power of the low pK_{a1}. It was observed that for ZrPs there are strong interdependencies between acidity of the product, unit cell volume, IR absorption, K_D, $k_{M/H}$ and k_M. Finally, it can be concluded that the ion exchange properties of α-ZrP products can be modified considerably by varying their synthesis conditions, perhaps to tailor specific actinide/lanthanide separations.

Keywords: Ion exchange, europium, americium, zirconium phosphate, inorganic synthesis, distribution coefficient, metal binding constant.

1 Introduction

Ongoing research worldwide on partitioning and transmutation (P&T) of spent nuclear fuel attempts to advance nuclear energy by multiple means. The research aims to maximize fission energy gain from bulk nuclear fuel while minimizing long term radiotoxicity of waste generated from spent nuclear fuel. According to the best case scenarios estimated for P&T, the high level waste radiotoxicity could be reduced by a factor of 100 [1].

Current partitioning methods include hydrometallurgical (e.g. UREX, PUREX) and pyrometallurgical methods used to separate either individual nuclides or groups of nuclides, e.g. fission products from actinides. The majority of current hydrometallurgical methods are based on solvent extraction, resulting in large amounts of secondary waste. The limited radiolytic stability of organic extractants is another drawback of solvent extraction. Inorganic materials offer generally a superior thermal and radiation resistance over organic counterparts. Ion exchange based on inorganic materials can offer an alternative or supporting methods that reduce the use of organic materials and solvents and minimize the volume of hazardous waste streams.

There are numerous studies done in the past on the ion exchange properties of zirconium bis(monohydrogen orthophosphate) monohydrate (α-ZrP) for mono- and divalent cations, with major contributions by G. Alberti and U.

***Corresponding author: Elmo W. Wiikinkoski,** Laboratory of Radiochemistry, Department of Chemistry, University of Helsinki, A.I. Virtasen aukio 1 (P.O. Box 55), FI-00014 Helsinki, Finland, E-mail: elmo.wiikinkoski@helsinki.fi
Risto O. Harjula, Jukka K. Lehto and Risto T. Koivula: Laboratory of Radiochemistry, Department of Chemistry, University of Helsinki, A.I. Virtasen aukio 1 (P.O. Box 55), FI-00014 Helsinki, Finland
Marianna L. Kemell: Laboratory of Inorganic Chemistry, Department of Chemistry, University of Helsinki, A.I. Virtasen aukio 1 (P.O. Box 55), FI-00014 Helsinki, Finland

Constantino, and A. Clearfield and Smith compiled in a review of that time [2]. Apart from the few studies [3] on ion exchange properties for Am, ZrP materials have not been studied with respect to separation of actinides from dissolved fuels or secondary waste streams. However, studies have shown that α-ZrP has a great selectivity towards trivalent americium and even greater towards trivalent europium [3, 4]. Thus α-ZrP was selected for further investigation on the topics of trivalent actinide and lanthanide removal from acidic media and their separation from each other.

α-ZrP is a well-known compound with a layered structure and composition $Zr(HPO_4)_2 \cdot H_2O$ [5]. It is a weakly acidic bifunctional compound and known to work as ion exchanger and binds light as well as heavy elements, e.g. alkali metals [6], Y^{3+}, La^{3+} and Ba^{2+} [7], Eu^{3+} and Am^{3+} [3, 4]. α-ZrP has been shown to retain its structure in conditions up to 500 °C and 13.3 mol·L^{-1} nitric acid [3] and after three MGy absorbed dose of ionizing radiation [8]. Other forms of ZrP include another layered structure γ-ZrP with composition $Zr(PO_4)(H_2PO_4) \cdot 2H_2O$, and τ-ZrP, which has three dimensional network structure and composition $Zr(HPO_4)_2$.

This study of several α-ZrP products, synthesized in different conditions, aims to develop hydrometallurgical separation methods based on the inorganic ion exchanger ZrP. Ideally these materials could separate either specific nuclides or groups of nuclides straight from spent nuclear fuel dissolved in nitric acid resulting in a more straightforward method free of organic solvents or additives. An alternative and perhaps more realistic use would be the treatment of secondary waste streams formed in current hydrometallurgical partitioning methods. Generally speaking, it is difficult to separate trivalent lanthanides and trivalent actinides from each other, since their chemistry is quite similar. The mentioned best case P&T scenarios involve the burning of trivalent actinides in modern reactor types, which would be inhibited by the presence of trivalent fission products. For this investigation, actinide Am^{3+} and lanthanide and Eu^{3+} was chosen to investigate the feasibility of separation, indicated by differences in selectivity, of such similar elements by the means of inorganic ion exchange.

2 Experimental section

2.1 Synthesis of materials

Three zirconium phosphate products (ZrP) were synthesized using different synthesis methods. The products thus obtained are abbreviated as ZrP A, ZrP B and ZrP C.

ZrP A was synthesized (adapted from García [9]) by dissolving 25 g of zirconium tetrachloride (Honeywell, Germany) in 430 mL of 2 mol·L^{-1} hydrochloric acid. This solution was slowly added to 400 mL of 1.25 mol·L^{-1} orthophosphoric acid while stirring continuously. The resulting white precipitate was washed multiple times with fresh 0.3 mol·L^{-1} orthophosphoric acid until the washing solution pH levelled off. After separating the final liquid, the white precipitate was then left to dry at room temperature.

ZrP B was synthesized (adapted from Alberti and Torracca [10]) by the so called HF-method. Eleven gram of zirconium oxychloride octahydrate (Merck Millipore, USA) was dissolved in 160 mL of water. While stirring rigorously, 8 mL of 40 % hydrofluoric acid was added, followed by 92 mL of 85 % orthophosphoric acid. The solution was left in stirring continuously under air flow overnight at room temperature. ZrP precipitated slowly as zirconium fluoride complexes broke down by evaporation of HF. The resulting white precipitate was washed multiple times with 0.3 mol·L^{-1} orthophosphoric acid until washing solution pH levelled off and it was left to dry at room temperature.

ZrP C was synthesized (adapted from Rajeh and Szirtes [11]) by a refluxing method. 6.4 g of zirconium oxychloride octahydrate (Merck Millipore, USA) was dissolved in 20 mL of water and 55 g of sodium dihydrogen phosphate monohydrate (Sigma-Aldrich, USA) was dissolved in 40 mL of 3 mol·L^{-1} hydrochloric acid. The latter was added drop wise to the former under constant stirring at 80 °C. The solution was then refluxed at 80 °C for 30 h and the resulting precipitate was left in its mother liquid for 2 days at room temperature. The precipitate was separated and washed with a total of 200 mL of 2 mol·L^{-1} orthophosphoric acid and further with ultrapure water until its pH levelled off at three. The white precipitate was separated and dried for 4 days in oven at 60 °C.

All synthesized ZrP products were ground and sieved to grain sizes between 0.074 and 0.149 mm.

2.2 Titration of ZrP products

The acid characters of products ZrP A, B and C were studied by base titration. The products were first preconditioned to H-form by equilibrating overnight in 0.1 mol·L^{-1} nitric acid. Thereafter they were washed with a small amount of water to remove excess acid until pH > 3, and dried in oven at 60 °C. The products were then added to 1 mol·L^{-1} $NaNO_3$ solution in polyethylene vials with the ratio of 100 mg to 19 mL. The role of $NaNO_3$ was to keep ionic strength constant during the experiment. Titration was done by adding a small volume of 1 mol·L^{-1} NaOH

and equilibrating for 1 day in a rotary mixer, followed by centrifugation and pH measurement before the next addition. When the third and final pH plateau characteristic to diprotic acids was reached, additions were halted. The total addition of NaOH was about 1.3 mL which corresponded to 13 mmol·g^{-1}, at which point equilibrium solution pH was from 11 to 12 depending on the product.

2.3 Determination of distribution coefficient

Am and Eu sorption of the materials as a function of pH was studied in 0.1 mol·L^{-1} $NaNO_3$ background solutions using a batch method. Separately, 10 mL of Am and Eu solutions, spiked with gamma-emitting $^{241}Am^{3+}$ and $^{152}Eu^{3+}$ tracers, was equilibrated in a rotary mixer with 20 mg of each ZrP material for 3 days in polyethylene vials. Thus the batch factor *V/m* in Eq. 6 (see Supplementary Information) was 500 L·kg^{-1}. The pH of the solution was adjusted with nitric acid. The tracers $^{241}Am^{3+}$ and $^{152}Eu^{3+}$ were obtained from New England Nuclear Corporation and Amersham Plc., respectively. After equilibrating, the mixtures were centrifuged at RCF 2600 g for 10 min and the solutions were filtered through 0.2 μm membrane syringe filters (Supor, Pall Corporation). Solution gamma activities were measured before (A_0) and after the equilibration (A) with WIZARD 1480 (PerkinElmer) sodium iodide gamma counter. Values of distribution coefficient K_D were then calculated from Eq. 6 (see Supplementary Information), for ^{152}Eu and ^{241}Am.

2.4 Characterization of ZrP products by X-ray powder diffraction, infrared transmittance, energy dispersive X-ray spectroscopy and scanning electron microscopy

To identify crystalline phases of the ZrP products their X-ray diffraction patterns were determined. XRD-measurements were carried on a Philips PW1820 powder diffractometer equipped with Philips PW1710 diffractometer control unit and Siemens Kristalloflex X-ray generator. Copper $K_{\alpha 1}$ X-rays of wavelength 1.54056 Å were used with a 2θ-angle step size of 0.040° and counting rate of 2.5 s per step over the total 2θ range of 7 to 70°. Unit cell parameters were calculated from using UnitCell software [12] developed by Tim Holland and Simon Redfern.

Infrared transmittances of the ZrP products over wavenumbers from 4000 to 650 cm^{-1} were measured with Spectrum One FTIR spectrometer (PerkinElmer) fitted with Universal ATR sampling accessory (PerkinElmer) and Spectrum software.

The morphology of the ZrP particles was studied with a Hitachi S-4800 field emission scanning electron microscope (FESEM). The P/Zr ratios were measured with an Oxford INCA 350 energy dispersive X-ray spectrometer (EDX) connected to the Hitachi S-4800 FESEM. Powder samples were attached to a carbon tape and excess particles were blown away with pressurized air flow.

3 Results and discussion

3.1 Crystalline phases, morphology and composition of prepared ZrP products

XRD measurements showed very similar diffraction patterns for all three ZrP products (Figure 1). All diffraction patterns corresponded to the well-known monoclinic crystal structure (space group P21/c) of α-zirconium phosphate ($Zr(HPO_4)_2 \cdot H_2O$) [5]. The unit cell volumes of the products decreased in the order ZrP A: 731.31(11) Å^3 > ZrP C: 727.69(11) Å^3 > ZrP B: 725.88(9) Å^3 (Table 1). The main difference between the spectra was in the intensities of the first peak at 11.7° 2θ-angle, which corresponds to an interlayer distance of 7.6 Å in the layered ZrP structure. This peaks intensity ratio for B:C:A was approximately 12:2:1, while the background ratio surrounding the peak was 1:1:1. As the crystals of products B and C have similar morphologies, the 6-fold difference in the intensities should not be consequence of differences in systematic orientations of the crystals. However, this could instead indicate that in crystals of product B, the ZrP layers themselves are aligned in a way that corresponding same elements sit on top of each other, intensifying the peak. Compared to product B, C would have a looser alignment and A would have the most staggered alignment. This difference in alignment would have impact on the cavities formed by adjacent ZrP layers and in that way could affect the ion exchange sites in the interlayer space. The cavities have been discussed and illustrated in the literature [5].

EDX analysis data indicated that the compounds had the same P:Zr ratio (average 2.43 ± 0.05) within the margin of uncertainty: 2.47 ± 0.05 for ZrP A, 2.37 ± 0.08 for B and 2.44 ± 0.09 for C. These ratios were determined as an average measurement covering 100 μm × 100 μm area containing numerous particles. SEM images of each product are shown in Figure 2. The images are not from the grain size fraction used in the sorption experiments but have

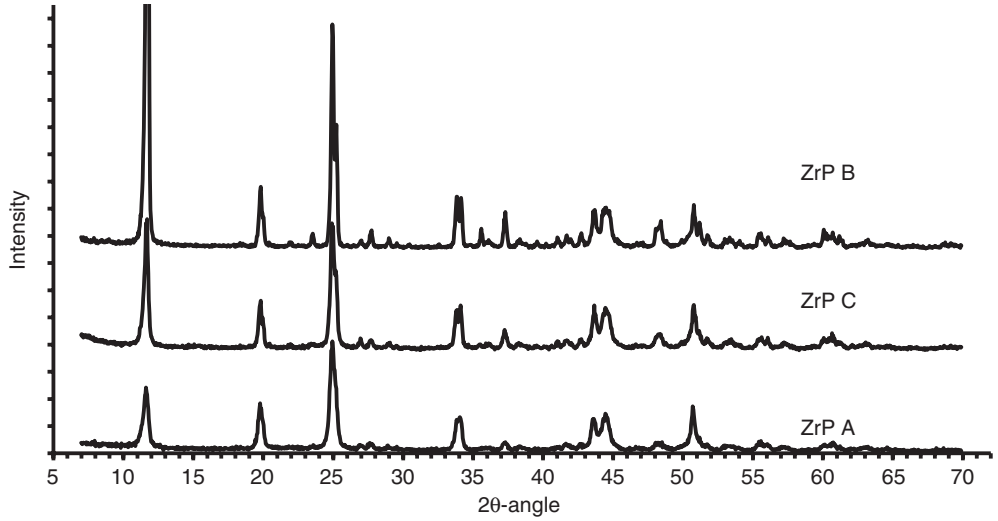

Figure 1: Powder XRD patterns of zirconium phosphate products ZrP A, B and C as a function of 2θ-angle with intensities in arbitrary units. The first peak of ZrP B at 11.7° is not shown in the figure as a whole: it's intensity ratio for B:C:A is approximately 12:2:1, while the ratio of background surrounding the peak is 1:1:1.

Table 1: Unit cell parameters (monoclinic, $\alpha=\gamma=90$ degrees) for ZrP-A, B and C.

	ZrP-A	Uncertainty (1σ)	ZrP-B	Uncertainty (1σ)	ZrP-C	Uncertainty (1σ)
a (Å)	9.1080	0.0008	9.0665	0.0008	9.0850	0.0007
b (Å)	5.2931	0.0006	5.2925	0.0006	5.2904	0.0006
c (Å)	16.334	0.003	16.259	0.002	16.275	0.003
β (°)	111.763	0.009	111.501	0.008	111.527	0.008
Cell vol. (Å³)	731.31	0.11	725.88	0.09	727.69	0.11

smaller grain size due to further grinding. From images for ZrP A (Figure 2a and b) we see wavy-shaped microstructures on the particle surfaces that are not found in other compounds. Also particle morphology is different and not plate-like, unlike in B and C. Some single point P:Zr ratio determinations for large ZrP A particles showed higher than average ratios: up to 2.8. These and other values above the theoretical value of two, derived from the ideal composition, could result from residual orthophosphoric acid in the products as suggested by García et al. [9]. Smaller particles of ZrP A are bound together in clusters, and apparently the plate-like form is lost. However, some of the ZrP A particles, as the one shown in Figure 2a, show plate-like structure similar to ZrP B and C although the plates are bound together in varying orientations. Figure 2c and d show plates of ZrP B. In (c) a side profile of a plate is shown, and clustering of small number of plates on top of each other can be seen here. This was typical for ZrP B and C but not on such a large scale as for A. Figure 2e shows a close-up of ZrP C plate cluster with similar growing of plates on top of each other than in (c), and (f) shows small plate distribution of C similar to the images of B.

3.2 Infra-red transmittance spectra of the ZrP products

IR transmittance for the ZrP products A, B and C (Figure 3) showed strong absorptions around 950 to 1100 cm^{-1}, attributed to vibrations of the orthophosphate group [13]. In this region, the obtained products differed greatly in their absorbance and therefore the peaks in the slightly varying range of 951 to 963 cm^{-1} were selected to explore possible correlation between the IR absorbance intensities of phosphate groups and the selectivity coefficient $\log k_{M/H}$ or acid dissociation constant pK_{a1}. This will be discussed later in the text and the result is shown in Figure 7. There were small variations in the exact peak positions for the products: 951, 957 and 963 cm^{-1} for A, B and C, respectively.

3.3 Titration of the ZrP products

Alkali titration curves for each studied products are shown in Figure 4. The inherent acid character of the

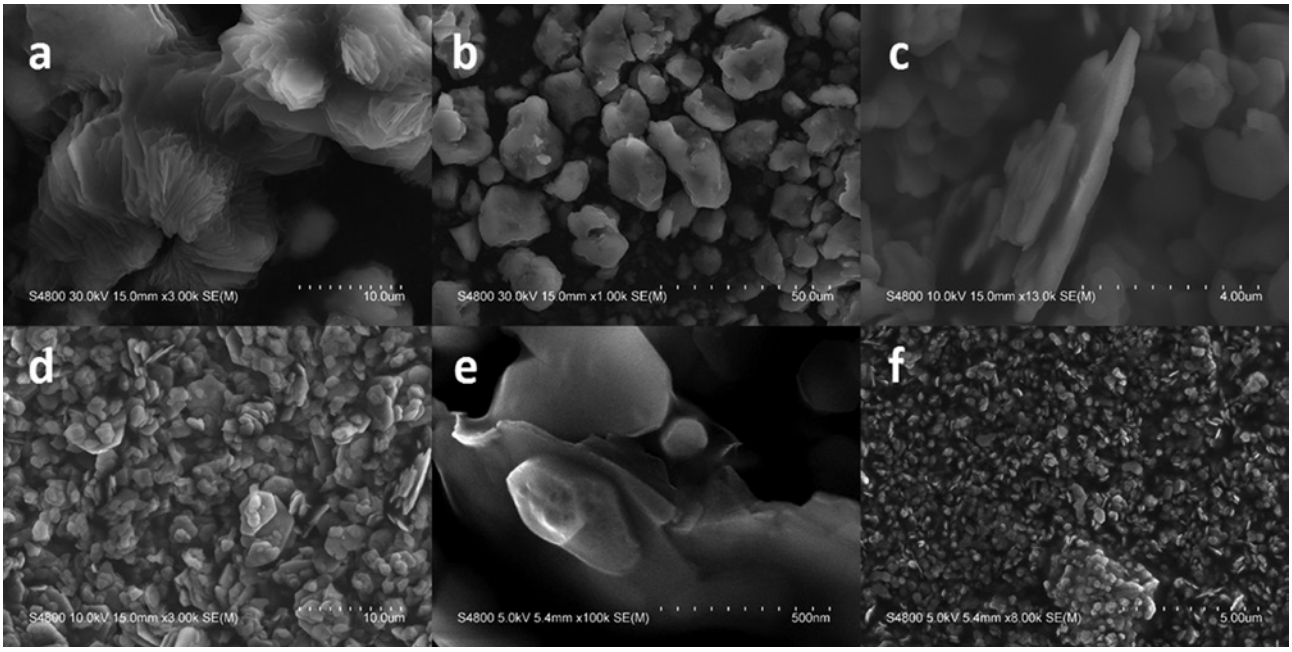

Figure 2: The morphology of the ZrP particles studied with a Hitachi S-4800 field emission scanning electron microscope. (a) Close-up of ZrP A, where plate-like microstructures similar to ZrP B and C are seen, but the plates are bound together with varying orientation. (b) Big clumps of ZrP A. (c) Close-up of ZrP B plates, with focus on a side profile of such plate. (d) Distribution of multiple plates in ZrP B. (e) Close-up on a particle of ZrP C. (f) View on ZrP C plates, which have similar morphology to ZrP B.

materials in H-form affects the pH upon immersion in water. When alkali is added to the system in the form of dilute NaOH solution, pH increases characteristic to the material in question. Based on Eq. 12 (see Supplementary Information) and taking into account the autodissociation of water, the conversion to the Na-form (q_{Na}, meq·g^{-1}) can be calculated from

$$q_{Na} = ([OH^-]_i - [OH^-] + [H_3O^+] - [H_3O^+]_i)(V/m),$$

where $[OH^-]_i$ refers to the added hydroxide and $[H_3O^+]_i$ to the initial pH before addition. $[OH^-]$ and $[H_3O^+]$ can be calculated from pH measured after equilibration. Earlier titration studies of crystalline ZrP have shown that it is diprotic in nature with equivalence points at NaOH consumption of about 3.3 meq·g^{-1} and 6.6 meq·g^{-1} [6, 14]. Calculated from the compositional formula $Zr(HPO_4)_2$ the concentration of hydronium ions in the compound is 6.6 meq·g^{-1} divided into two fractions with varying

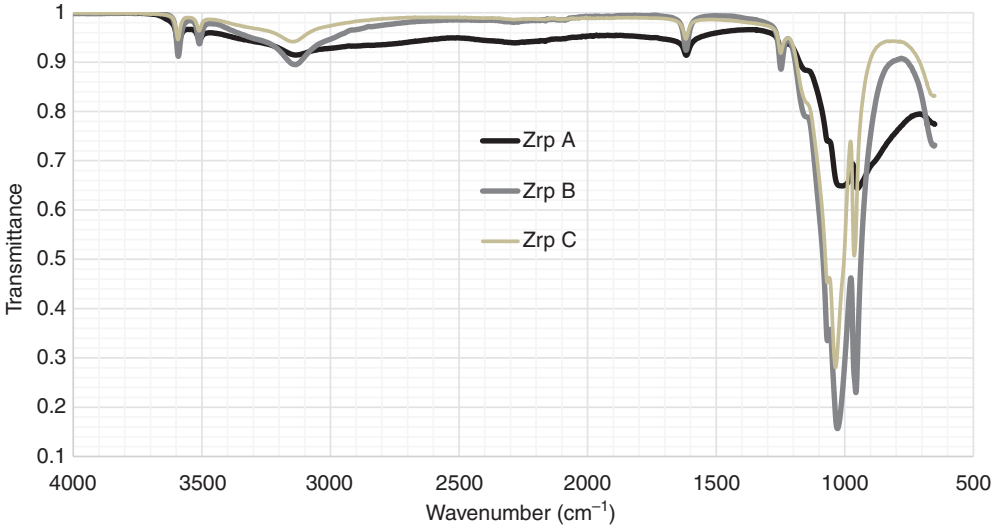

Figure 3: IR transmittance spectra for zirconium phosphate products A, B and C.

acidity. In this study, ZrP C did not show any clear equivalence points (Figure 4). ZrP A and B showed an equivalence point at NaOH-consumption of about 6.6 meq·g^{-1} in line with earlier studies. This equivalence point evidently corresponds to the dissociation of the second OH-group attached to the phosphorus (pK_{a2}). However, no equivalence points were observed at 3.3 meq·g^{-1} that would correspond the half-titrated ZrP. Instead, for ZrP B an equivalence point at about 2.2 meq·g^{-1} and for ZrP A at about 4 meq·g^{-1}, could be seen. Thus the products show diprotic nature but the fractions of the two weakly acidic sites are not equal. Similar behaviour has been observed earlier e.g. in the titration of ZrP with LiOH with equivalence points at about 5 and 6.6 meq·g^{-1} [14]. However, while numerous titration studies of ZrP have been carried out [6, 14–16], no numerical values of the pK_a-values have been determined in those studies.

The level of pH-values in the early stages of titrations (Na-conversion 0-2 meq·g^{-1}) in the ZrPs increased in the order ZrP B < ZrP C < ZrP A (Figure 4). The acidity of the products thus increased in the reverse order: ZrP A < ZrP C < ZrP B. The pK_a-value of the first, more acidic POH-groups (pK_{a1}) was estimated from Eq. 11 (see Supplementary Information) using the theoretical value Q_1 of 3.3 meq·g^{-1} for the capacity of these groups. At $\beta = 0.5$ (1.65 meq·g^{-1}) the pH-values corresponding to pK_{a1}-values of the products were 3.5 for ZrP A, 2.3 for ZrP B and 3.1 for ZrP C, from Figure 4.

Possible correlation between the acquired pK_{a1}-values and various other numerical results were investigated and are reported as Pearson's correlation coefficient r. It was found that there is significant negative correlation between pK_{a1}-values of the products and their IR absorption at approximately 960 cm^{-1}: $r = -0.999$, $p < 0.01$. Positive correlation between pK_{a1} and unit cell size is possible, but the uncertainty for this is very high due to the low number of data points (3): $r = 0.929$, $p = 0.24$.

3.4 Eu and Am uptake by ZrP products

The determined logarithms of distribution coefficients K_D for Eu and Am were linear functions of pH (Figure 5 and Table 2). In each of the products A, B and C, the level of K_D was higher for Eu than for Am. The Eu and Am sorption started to increase with increasing pH in the order of increasing K_D: ZrP A > ZrP C > ZrP B. The fitted slopes of the log K_D vs. pH curves were in the range of 3.4-2.3. Ideally, as seen from Eq. 5 (see Supplementary Information) the slope for Am^{3+}/Eu^{3+} for hydronium exchange is +3 and thus the observed values were fairly consistent with trivalent metal for hydronium ion exchange even though rather large variations were observed. Values lower than three might be explained by possible co-exchange of divalent Am and Eu nitrate species as calculations with PHREEQC program showed that at pH 1–6 25–40 % of Am was present as $Am(NO_3)^{2+}$. The corresponding presence of $Eu(NO_3)^{2+}$ was 10–15 %. Very high (>10^6) and very low (<5) K_D values were omitted from calculations, as their uncertainties were great. This was because the solution activities in case of very high K_D values were roughly equal to background, and in the case of very low K_D values, roughly equal to the

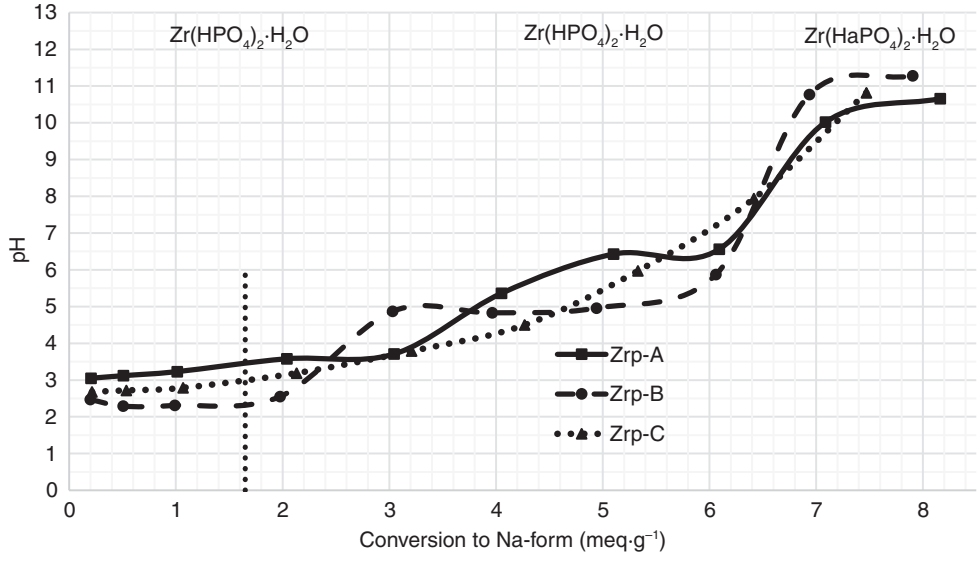

Figure 4: Alkali titration curve for ZrP A, B and C. The approximate of acid constant pK_{a1} is determined graphically as the pH of curve value at 1.65 meq · g^{-1}, indicated here as the vertical line. The composition of prevailing species in different pH areas are indicated on the top.

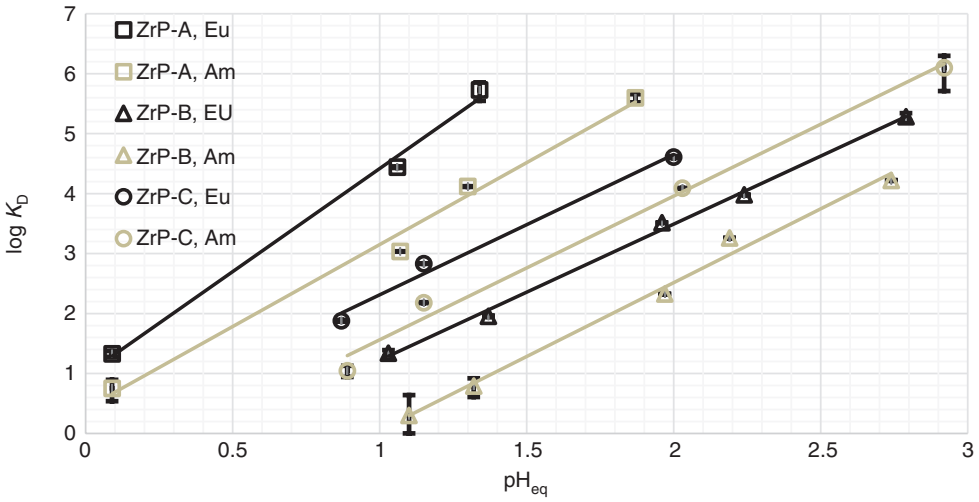

Figure 5: Distribution coefficients K_D for Eu and Am sorption on zirconium phosphates A, B and C as a function of equilibrium pH.

Table 2: Linear regression parameters for $y = ax + b$, where y is log K_D and x is pH in equilibrium.

Product, nuclide	a	b	R^2
ZrP A, Eu	3.4385	0.9789	0.9946
ZrP A, Am	2.7335	0.4161	0.9898
ZrP B, Eu	2.2696	−1.0482	0.9971
ZrP B, Am	2.4629	−2.4109	0.9902
ZrP C, Eu	2.3392	−0.0275	0.9878
ZrP C, Am	2.3966	−0.8349	0.9906

initial activities. The omitted data points were for ZrP A at pH 2–3, for ZrP B at pH 0 and for ZrP C at pH 0, 0.5 and 3.

In comparison to analogous studies done in the past, K_D results for Am^{3+} seem to be in line with the product ZrP B. Mimura and Akiba [3] has done batch experiments in almost equal conditions (300 *V/m*, 0.1 M $NaNO_3$) with powderous α-ZrP as well as silica granulated α-ZrP. Interpolated from their line for powderous product, K_D at pH_{eq} 1.5 was 20; at pH_{eq} 2 was 300 and at pH_{eq} 2.4 was 3000. These are, within 10 %, the same results that we got for ZrP B. For Eu^{3+} however, the similar studies [4] were reported only for silica granulated α-ZrP, which has approx. one order of magnitude lower values than ZrP B.

Whereas a large difference in Eu and Am sorption, meaning a larger separation factor, is favourable for separation purposes, all three products could be usable, just at different pH ranges. Separation factors, defined as the ratios of the distribution coefficients K_D(Eu): K_D(Am), ranged from 4 to 41 for ZrP A, from 5 to 15 for B, and from 3 to 7 for C.

The selectivity coefficients of Eu/H and Am/H exchange for the ZrPs were determined from the intercepts (IC) of the linear regressions of log K_D vs. pH plots (Figure 5). It is obtained [17] from Eq. 5 (see Supplementary Information) that

$$\log k_{A/B} = \mathrm{IC} - z_A \log Q$$

where B is H^+, A is Eu^{3+} or Am^{3+} and therefore z_A is 3, and Q is 6.6 meq·g^{-1}. The determined selectivity coefficients are tabulated with the pK_{a1} values of the ZrPs in Table 3. There was a clear linear trend of selectivity coefficients of both Eu and Am with pK_{a1} on a logarithmic scale (Figure 6). The selectivity of the ZrPs for Eu and Am increased with increasing pK_{a1}-value. Thus the selectivities increased with decreasing acidity of the products. The positive correlation between pK_{a1} and log $k_{M/H}$ is strong, as $r = 0.982$ and $p = 0.12$ for Eu, and $r = 0.992$ and $p = 0.08$ for Am, but the uncertainty is high in both cases due to the low number of data points.

IR absorbances related to phosphate group vibrations (see before) increase in the order ZrP A < C < B, which is the same order that the selectivity coefficients $k_{M/H}$ and pK_{a1} decrease (Figure 7). More absorbance in this region is related to more abundance of phosphorous groups of this character, therefore along with increased absorbance the acidity increases and selectivity decreases.

Table 3: pK_{a1}-values, selectivity coefficients ($k_{M/H}$) for Eu/H and Am/H exchange and metal binding coefficients (k_M) for Eu and Am in ZrP A, B and C.

Product	pK_{a1}	log $k_{Eu/H}$	log $k_{Am/H}$	log k_{Eu}	log k_{Am}
ZrP A	3.5	−1.48	−2.04	9.02	8.46
ZrP B	2.3	−3.51	−4.87	3.39	2.03
ZrP C	3.1	−2.49	−3.29	6.81	6.01

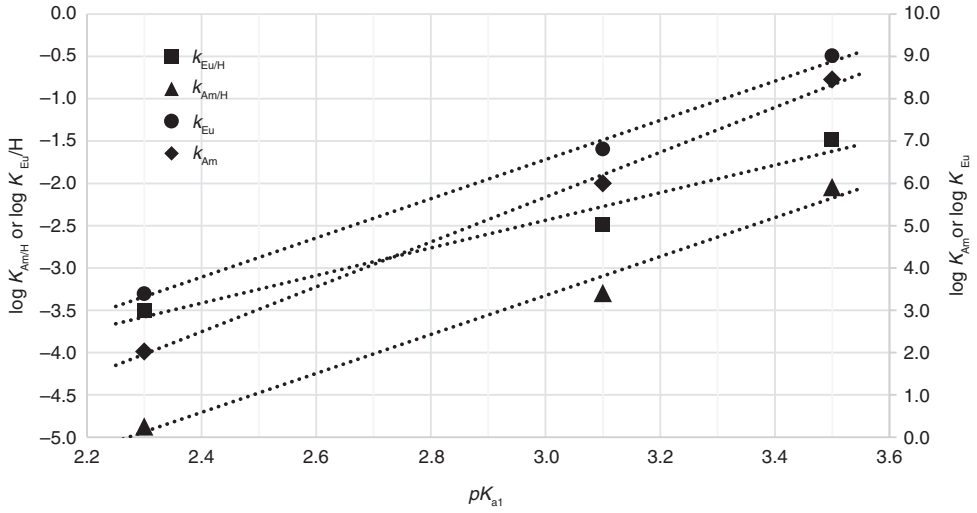

Figure 6: Acid constant pK_{a1} vs. selectivity coefficient $k_{M/H}$ and metal binding coefficient k_M (M = Eu or Am) for ZrP A (right), B (left) and C (middle).

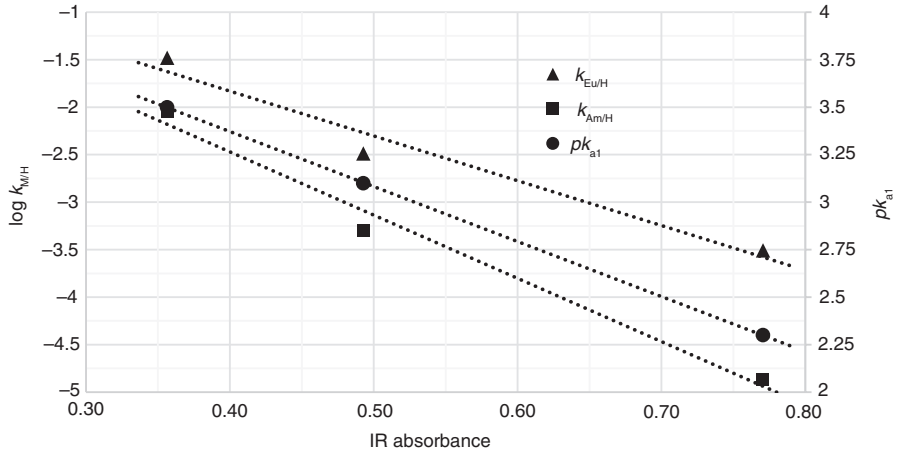

Figure 7: Selectivity coefficients $k_{M/H}$ (M = Eu or Am) and acid constant pK_{a1} vs. IR absorbance at sharp peak at 951, 957 and 963 cm^{-1} for ZrP A (left), B (right) and C (middle) respectively.

Considering that the ZrPs had high Eu and Am uptake values in acidic solution, the values of $k_{Eu/H}$ and $k_{Am/H}$ appear very low. This can be explained by the weak acidity of the ZrP products. The selectivity coefficient as formulated in Eq. 2 (see Supplementary Information) contains two reactions. First, the dissociation of the OH-group; i.e. $POH \rightleftharpoons PO^- + H^+$ and second, binding of the metal in the PO^--group, i.e. $3\,PO^- + M^{3+} \rightleftharpoons M(PO)_3$, which can be characterized by metal binding coefficient k_M. It is obtained (see Supplementary Information) in logarithmic form that

$$\log k_M = \log k_{M/H} + 3\,pK_a$$

The metal binding coefficients derived showed very high values up to about 10^9 (Table 3) and increased linearly with pK_{a1} values in a logarithmic scale (Figure 6). There is significant positive correlation between pK_{a1} and metal binding coefficient log k_M: $r = 0.997$ and $p = 0.05$ for Eu, and $r = 0.998$ and $p = 0.04$ for Am. Binding thus increased strongly as the acidity decreased. The selectivity coefficients $k_{M/H}$ had low values as in the case of trivalent metal exchange, as they depend on the third power of K_a-values that are much smaller than unity. For the three ZrP products of the same bulk structure and composition, according to XRD and EDX, the metal binding coefficients differ remarkably.

4 Conclusions

All the investigated ZrP products in this work were found to have the crystal structure of α-zirconium phosphate. While crystal structure and composition of all synthesized compounds are similar according to XRD and EDX results, distribution coefficients for both Am and Eu vary greatly for each compound. The main observed differences in crystal structure are unit cell volumes and the alignment of adjacent ZrP layers. Unit cell volume increases in the order of ZrP B < C < A, which is the same order that pK_{a1} increases and therefore the acidity decreases: ZrP B > C > A. The intensity of the first peak in XRD spectra, corresponding to the diffraction due to adjacent ZrP layers, was greatly enhanced in the order ZrP A < C < B. It was deduced from the morphology similarities of B and C that possible systematic orientation of the crystals should not be the major factor in the first peak intensity differences. Instead, it could mean that in B, equal atoms in the structure sit closer to being on top of each other in adjacent layers. In ZrP A, zirconium atom of one layer would be closer to being on top of a phosphorus atom in the adjacent layer, and in ZrP C, the situation is somewhere between. This alignment would have impact on the cavities formed by the adjacent layers. In these cavities are located the water molecules and also the exchangeable hydrogen. Therefore, it would be likely for these alignment differences to have an impact on the differences of ion exchange properties in these products.

As IR absorbance related to phosphate group vibrations (at approx. 960 cm^{-1}) increased in the order ZrP A < C < B, pK_{a1} decreased, i.e. acidity increased. FESEM investigations were made to determine via EDX module the P:Zr-ratios and to try to explain varying acidities. The ratios turned out to be, considering the acceptable uncertainty of 2 to 4 %, identical for all the compounds. It is unclear in which manner the phosphorus is distributed if the phosphorus content is indeed identical in the products.

As acidity increased, the selectivity coefficients and sorption strength decreased. Metal binding coefficients were of high value, especially in ZrP C and A (up to 10^9), while the selectivity coefficients were low (10^{-5} to 10^{-1}), because they are related to the third power of the low acid dissociation constants.

Distribution coefficients for both Eu and Am increased in the order of ZrP C < B < A, with a higher value always for Eu. Whereas a large difference in Eu and Am sorption (meaning a larger separation factor) is favourable for separation purposes, all three products could be usable for separation, in different pH areas. Separation factors, defined as K_D(Eu): K_D(Am), were: from 4 to 41 for ZrP A, from 5 to 15 for B, and from 3 to 7 for C.

The results are very interesting because ZrP products seem to lend themselves for adjusting their acidity and thus their metal binding properties. Further investigation will include fine tuning synthesis conditions in one selected synthesis route, and looking at the outcome related to distribution coefficients. Preliminary column experiments have been conducted and further column loading and elution tests will be carried out and reported later.

Acknowledgements: The research is partly funded by State Nuclear Waste Management Fund, on the basis of proposals by the Ministry of Employment and Education of Finland. It is part of Finnish Research Programme on Nuclear Waste Management which is based on the Nuclear Energy Act (990/1987). Authors would like to thank the Laboratory of Polymer Chemistry, Department of Chemistry, University of Helsinki, for the use of FTIR instrumentation.

References

1. Accelerator-driven Systems (ADS) and Fast Reactors (FR) in Advanced Nuclear Fuel Cycles. OECD Nuclear Energy Agency, Paris (2002).
2. Alberti, G., Constantino, U.: Recent progress in the field of synthetic inorganic exchangers having a layered or fibrous structure. J. Chromatogr. **102**, 5 (1974).
3. Mimura, H., Akiba, K.: Adsorption behavior of americium on granulated zirconium phosphate. J. Nucl. Sci. Technol. **32**, 819 (1995).
4. Mimura, H., Akiba, K.: Adsorption properties of europium on granulated α-zirconium phosphate. J. Nucl. Sci. Technol. **33**, 592 (1996).
5. Clearfield, A., Smith, G. D.: The crystallography and structure of α-zirconium bis(monohydrogen orthophosphate) monohydrate. Inorg. Chem. **8**, 431 (1969).
6. Clearfield, A.: Inorganic ion exchangers with layered structures. Ann. Rev. Mater. Sci. **14**, 205 (1984).
7. Möller, T., Bestaoui, N., Wierzbicki, M., Adams, T., Clearfield, A.: Separation of lanthanum, hafnium, barium and radiotracers yttrium-88 and barium-133 using crystalline zirconium phosphate and phosphonate compounds as prospective materials for a Ra-223 radioisotope generator. Appl. Radiat. Isotopes. **69**, 947 (2011).
8. Szirtes, L., Lázár, K., Kuzmann, E.: Effect of ionizing radiation on various zirconium phosphate derivatives. Radiat. Phys. Chem. **55**, 583 (1999).
9. Trobajo, C., Khainakov, S. A., Espina, A., García, J. R.: On the synthesis of α-zirconium phosphate. Chem. Mater. **12**, 1787 (2000).

10. Alberti, G., Torracca, E.: Crystalline insoluble salts of polybasic metals - II. Synthesis of crystalline zirconium or titanium phosphate by direct precipitation. J. Inorg. Nucl. Chem. **30**, 317 (1968).
11. Rajeh, A. O., Szirtes, L.: Investigations of crystalline structure of gamma-zirconium phosphate. J. Radioanal. Nucl. Chem. **195**, 319 (1995).
12. Holland, T. J. B., Redfern, S. A. T.: Unit cell refinement from powder diffraction data; the use of regression diagnostics. Mineral. Mag. **61**, 65 (1997).
13. Horsley, S. E., Nowell, D. V., Stewart, D. T.: The infrared and Raman spectra of α-zirconium phosphate. Spectrochim. Acta **30A**, 535 (1974).
14. Harvie, S. J., Nancollas, G. H.: Ion exchange properties of crystalline zirconium phosphate. J. Inorg. Nucl. Chem. **32**, 3923 (1970).
15. Clearfield, A., Duax, W. L., Medina, A. S., Smith, G. D., Thomas, J. R.: On the mechanism of ion exchange in crystalline zirconium phosphates. I. Sodium ion exchange of α-zirconium phosphate. J. Phys. Chem. **73**, 3424 (1969).
16. Clearfield, A., Troup, J.: On the mechanism of ion exchange in crystalline zirconium phosphate. II. Lithium ion exchange of α-zirconium phosphate. J. Phys. Chem. **74**, 314 (1970).
17. Harjula, R.: Ion Exchange Theory. In: I. D. Wilson, C. F. Poole, T. R. Adlard, M. Cooke (Eds.), Encyclopedia of Separation Science, Vol. 2. London (2000), Academic Press, p. 1651.

Supplemental Material: The online version of this article (DOI: 10.1515/ract-2016-2740) offers supplementary material, available to authorized users.